Experimental demonstration of multi-aperture digital coherent combining over a 3.2-km free-space link

Experimental demonstration of multi-aperture digital coherent combining over a 3.2-km free-space link

D. J. Geisler, T. M. Yarnall, C. M. Schieler, M. L. Stevens, B. S. Robinson, et al.

D. J. Geisler, T. M. Yarnall, C. M. Schieler, M. L. Stevens, B. S. Robinson, S. A. Hamilton, "Experimental demonstration of multi-aperture digital coherent combining over a 3.2-km free-space link," Proc. SPIE 10096, Free-Space Laser Communication and Atmospheric Propagation XXIX, 100960C (24 February 2017); doi: 10.1117/12.2256581

SPIE.

Event: SPIE LASE, 2017, San Francisco, California, United States

Invited Paper

Experimental Demonstration of Multi-Aperture Digital Coherent Combining Over a 3.2-km Free-Space Link

D. J. Geisler, T. M. Yarnall, C. M. Schieler, M. L. Stevens, B. S. Robinson, and S. A. Hamilton

Massachusetts Institute of Technology Lincoln Laboratory
244 Wood Street, Lexington, MA, USA 02420

ABSTRACT

The next generation free-space optical communications infrastructure will need to support a wide variety of space-to-ground links. As a result of the limited size, weight, and power on space-borne assets, the ground terminals need to scale efficiently to large collection areas to support extremely long link distances or high data rates. Recent advances in integrated digital coherent receivers enable the coherent combining (i.e., full-field addition) of signals from several small apertures to synthesize an effective single large aperture. In this work, we experimentally demonstrate the coherent combining of signals received by four independent receive chains after propagation through a 3.2-km atmospheric channel. Measured results show the practicality of coherently combining the four received signals via digital signal processing after transmission through a turbulent atmosphere. In particular, near-lossless combining is demonstrated using the technique of maximal ratio combining.

Keywords: free-space optical communication, coherent combining, digital signal processing

1. INTRODUCTION

Many space-borne systems need increasingly high-bandwidth connectivity to the ground in a limited size, weight, and power (SWaP) package to fulfill their missions. Free-space optical (FSO) communication systems demonstrations have already shown the utility of using the bandwidth-rich infra-red spectrum to achieve high data rate communications from low-SWaP space platforms to the ground in a variety of scenarios.[1–3] Further increases to the throughput of FSO communication systems typically require an increase in the signal power delivered to the receiver. SWaP limitations on space-borne platforms preclude significant increases in transmitter power or aperture diameter; therefore, further improvements are achieved by increasing the capability of the ground terminal. Increasing the collection area of the ground terminal while keeping all other performance metrics constant is an obvious way to increase the received power; however, increasing the diameter of an optical telescope beyond a few 10's of centimeters is both difficult and costly.[4] Furthermore, when the diameter is larger than the atmospheric coherence length, efficiently coupling the wavefront to single-mode fiber requires an adaptive optics system.

In our previous work, we identified a ground architecture based on an array of small telescopes.[5] That work included a laboratory demonstration of combining signals from each element of this array in a lossless manner over a significant range of input powers by using coherent detection and digital signal processing techniques. In practice, free-space optical communication through the atmosphere must contend with the unwanted effects of atmospheric turbulence.[6] Foremost among these effects is channel fading, whereby the received power can fluctuate by many orders of magnitude over millisecond-class time scales.[7] Channel fading can arise from amplitude distortions in the wavefront (scintillation) and also from turbulence-induced coupling losses that may occur when the receiver aperture is larger than the atmospheric coherence length.

In this paper, we provide an experimental demonstration of digital coherent aperture combining in the presence of atmospheric fading through a 3.2-km free-space link. Section 2 describes the architecture and signal

This work was sponsored by the Assistant Secretary of Defense for Research and Engineering under Air Force Contract #FA8721-05-C-0002. Opinions, interpretations, conclusions, and recommendations are those of the authors and are not necessarily endorsed by the United States Government.

Free-Space Laser Communication and Atmospheric Propagation XXIX, edited by Hamid Hemmati, Don M. Boroson,
Proc. of SPIE Vol. 10096, 100960C · © 2017 SPIE · CCC code: 0277-786X/17/$18 · doi: 10.1117/12.2256581

model for a multi-aperture coherent combining based receiver. Specifically, Section 2 details an analytical method for implementing maximal ratio combining in a fading channel environment, a technique that is commonplace in the radio-frequency realm (e.g., Ref. 8). Section 3 presents the experimental arrangement, which includes the hardware setup and the digital signal processing. Section 4 includes the experimental results for multi-aperture coherent combining over a 3.2-km free-space link. Finally, Section 5 concludes the paper by summarizing the findings of this work and speculates on potential future applications.

2. SYSTEM ARCHITECTURE

This section describes a multi-aperture system architecture for free-space optical communication that uses digital-domain coherent combining to synthesize a single signal from multiple received signals. After describing the system elements and a signal model, we review the lossless nature of maximal ratio combining.

2.1 Architecture and signal model

In preparation for processing and analyzing the signals captured in the free-space link experiment, we consider the system depicted in Figure 1. At the transmitter, a single complex waveform $x(t)$ is modulated onto an optical beam that propagates through an atmospheric channel. Turbulence in the atmospheric channel induces time-varying distortions in the propagating field in the form of phase-front distortion and also amplitude distortion (i.e., scintillation). At the receiver, K apertures with front-end optics are used to couple the wavefront to fiber, potentially applying tilt-correction or higher-order adaptive optics to increase the coupling efficiency. Because the various receivers detect noisy versions of the same transmitted waveform after atmospheric propagation, the communication channel is a SIMO (single-input, multiple-output) channel.

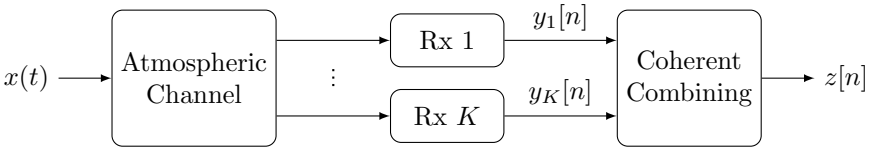

Figure 1: System block diagram. A transmitted waveform $x(t)$ is received by K front-end digital receivers. The digital signals $y_1[n], \ldots, y_K[n]$ are coherently combined to form a composite signal $z[n]$.

Behind each aperture, a coherent heterodyne detector uses a common local oscillator (LO) to down-convert an optical signal to electrical in-phase (I) and quadrature (Q) signals at some intermediate frequency. The intermediate frequency is such that the baseband signal bandwidth shifted by the intermediate frequency resides entirely within the sampling bandwidth of subsequent analog-to-digital converters. The noise internal to each of the receivers is modeled as additive white gaussian noise (AWGN); we choose this model to reflect our experimental arrangement wherein the fiber signals are preamplified before being mixed with the LO.

After coherent detection and sampling, the discrete-time I and Q signals from the K receiver branches are combined in digital signal processing (DSP) to produce a single signal for further demodulation. Our model for the K complex-valued signals fed to the DSP is given by

$$y_k[n] = h_k[n]c[n] + \nu_k[n], \quad k = 1, \ldots, K \tag{1}$$

where:

- $h_k[n]$ is a complex-valued random fading process that summarizes the multiplicative noise in the atmospheric channel due to scintillation and coupling imperfections at the kth receiver.
- $c[n]$ is the signal that is common to all K receivers, consisting of the transmitted baseband waveform and a down-converted local oscillator signal:

$$c[n] = x[n]e^{j(\omega n T_s + \phi[n])} \tag{2}$$

where T_s is the sampling period, $x[n] = x(nT_s)$, ω is the intermediate frequency (IF), and $\phi[n]$ is LO phase noise. For the remainder of the paper, we assume that $|x(t)| = 1$ for all t.

- $\nu_k[n]$ is complex additive white Gaussian noise (AWGN) in the kth coherent receiver. The noise in the I and Q dimensions is uncorrelated and each have variance σ_k^2. Additionally, the additive noise terms in the K different branches are assumed to be uncorrelated with each other.

For notational convenience, (1) can be written in terms of vector-valued signals:

$$\mathbf{y}[n] = c[n]\mathbf{h}[n] + \boldsymbol{\nu}[n], \quad \mathbf{y}, \mathbf{h}, \boldsymbol{\nu} \in \mathbb{C}^{K\times 1} \tag{3}$$

where $\mathbb{C}^{K\times 1}$ is the space of K-dimensional complex column vectors.

2.2 Coherent combining

The ability to coherently combine signals in the digital domain alleviates the complexity of hardware-based combining approaches (e.g., using optical phase-locked loops), providing a way to scale to systems with large numbers of apertures. The signal alignment requirements for using digital coherent combining are dictated by the bandwidth of $x(t)$, the underlying baseband waveform, whereas combining in the optical domain requires alignment precision to within a fraction of the wavelength of the light.

In this work, we restrict attention to linear combining techniques that use a time-varying, vector-valued weighting

$$\mathbf{w}[n] = [w_1[n], \ldots, w_K[n]]^{\mathsf{T}} \in \mathbb{C}^{K\times 1} \tag{4}$$

to form a composite signal

$$z[n] = \mathbf{w}[n]^{\mathsf{T}}\mathbf{y}[n], \tag{5}$$

where $(\cdot)^{\mathsf{T}}$ denotes transposition. A dynamic weighting $\mathbf{w}[n]$ is used to adapt to the time-varying nature of the atmospheric fading.

We will use signal-to-noise ratio (SNR) to evaluate the efficacy of the digital combining when the experimental results are presented in Section 4. SNR is the ratio of the signal power to the total noise power, i.e., the noise power in both complex dimensions. Because the atmospheric fading process $\mathbf{h}[n]$ is random and time-varying, the SNR of the received signals is also random and time-varying. The SNR in the kth receiver at sample n is defined as

$$\rho_k[n] \triangleq \frac{|h_k[n]c[n]|^2}{2\sigma_k^2} = \frac{|h_k[n]|^2}{\mathbb{E}|\nu_k|^2}, \tag{6}$$

where $\mathbb{E}$ denotes expectation with respect to the distribution of ν_k. Similarly, the SNR of the composite signal is defined as

$$\rho_{\mathbf{z}}[n] \triangleq \frac{\left|\mathbf{w}[n]^{\mathsf{T}}\mathbf{h}[n]\right|^2}{\mathbb{E}\left|\mathbf{w}[n]^{\mathsf{T}}\boldsymbol{\nu}[n]\right|^2}. \tag{7}$$

2.3 Maximal ratio combining

It is well-known that maximal ratio combining is the linear combining technique that maximizes the SNR of the composite signal (e.g., see Ref. 9). In maximal ratio combining, the optimal weight vector is given by

$$\mathbf{w}[n] = \left[\frac{\overline{h}_1[n]}{2\sigma_1^2}, \ldots, \frac{\overline{h}_K[n]}{2\sigma_K^2}\right]^{\mathsf{T}}, \tag{8}$$

where $\overline{(\cdot)}$ denotes complex conjugation. For this choice of $\mathbf{w}[n]$ or any scalar multiple thereof, it can be shown via the Cauchy-Schwarz inequality that the resulting SNR of the composite signal is optimal and is equal to the sum of SNRs of the constituent signals, i.e.,

$$\rho_{\mathbf{z}}[n] = \sum_k \rho_k[n]. \tag{9}$$

In principle, (9) shows that a single-aperture system can be split into a K-aperture system without any loss in performance by carrying out the following:

1) *Ensure that the total average power-in-fiber summed across the K branches is equal to the average power-in-fiber of the single aperture system.* While this could be achieved by scaling down and replicating the optics of the single-aperture system, the complexity of the optics can potentially be reduced depending on the size of the apertures and the characteristics of the atmospheric turbulence (in particular, the Fried parameter r_0). For example, it may be possible to replace a large aperture employing tilt-tracking and higher order adaptive optics with multiple small apertures employing only tilt-tracking while maintaining (or perhaps exceeding) the total power-in-fiber.

2) *Replicate the coherent receiver front end in all branches.* This may place a practical upper bound on the number of individual apertures that can be supported in a realistic system due to the cost of each front end.

3) *Perform maximal ratio combining in DSP.* Note that to implement maximal ratio combining in practice using the optimal weight vector in (8), one must have knowledge of the fading amplitude vector $\mathbf{h}[n]$ and the receiver noise variances $\{\sigma_k\}$. If the coherent receivers are identical, the noise variances will be equal and an optimal weighting is given by $\mathbf{w}[n] = \overline{\mathbf{h}[n]}$. However, $\mathbf{h}[n]$ is a random process that must be estimated in some manner, potentially leading to a performance penalty. The issue of estimating $\mathbf{h}[n]$ will be addressed later in Section 3.2.

3. EXPERIMENTAL ARRANGEMENT

This section describes the hardware arrangement and digital signal processing steps necessary for implementing a 1.6-km (3.2-km round-trip) atmospheric channel demonstration of multi-aperture coherent combining. This arrangement implements the system model from Section 2.

3.1 Hardware Arrangement

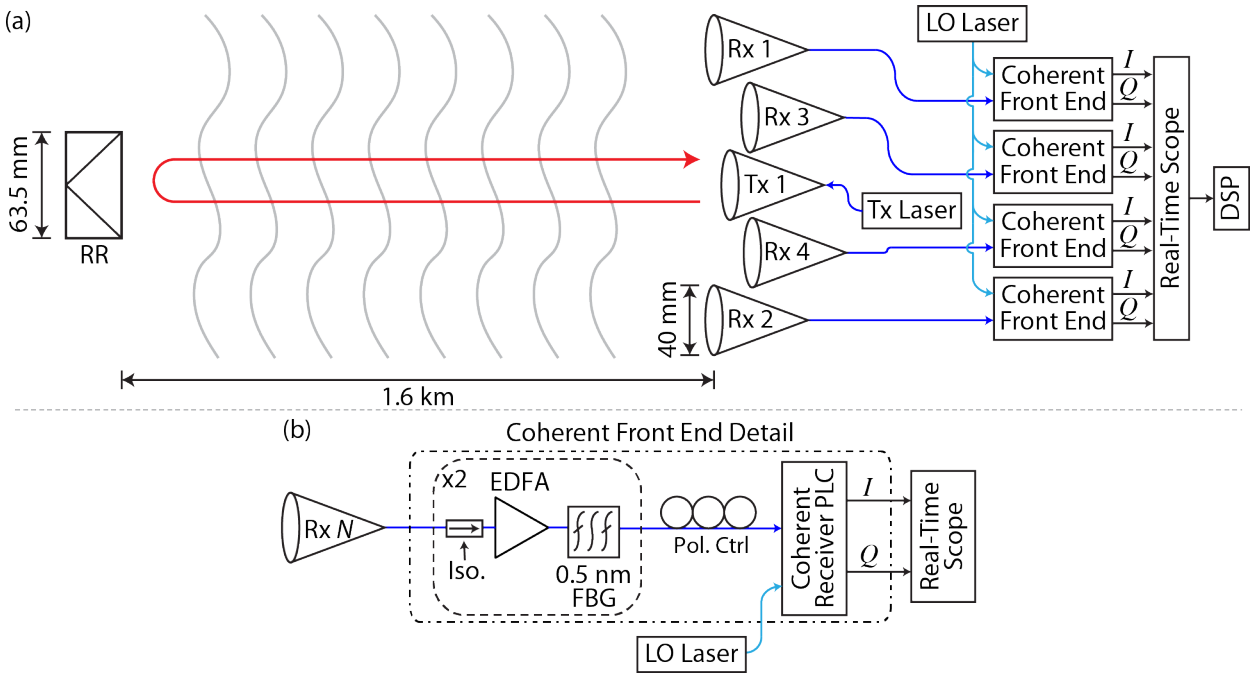

Figure 2: (a) Experimental arrangement. (b) Coherent front-end detail. RR: retro-reflector. Iso.: isolator. FBG: fiber Bragg grating. PLC: photonic lightwave circuit.

Figure 2 shows the experimental arrangement. As shown in Figure 2a, a 40-mm transmit aperture was co-bore-sighted with four 40-mm receive apertures. The transmit signal consisted of a continuous-wave (CW) laser. Upon transmission through the Tx 1 aperture, the signal propagated 1.6 km through the turbulent atmosphere

to a 63.5-mm retro-reflector, and then returned 1.6 km to the four receive apertures (solid red path in Figure 2). Each of the received signals underwent demodulation in parallel coherent front-ends (Figure 2b). The front-ends each down-converted the signal to the IF using a common LO, and provided the I and Q components of the signal at the IF for digitization using a real-time digital oscilloscope. Specifically, each coherent front-end had two stages of amplification and filtering followed by a photonic lightwave circuit that consisted of a 90° optical hybrid, balanced photodiodes, and trans-impedance amplifiers (see Ref. 5 for further details).

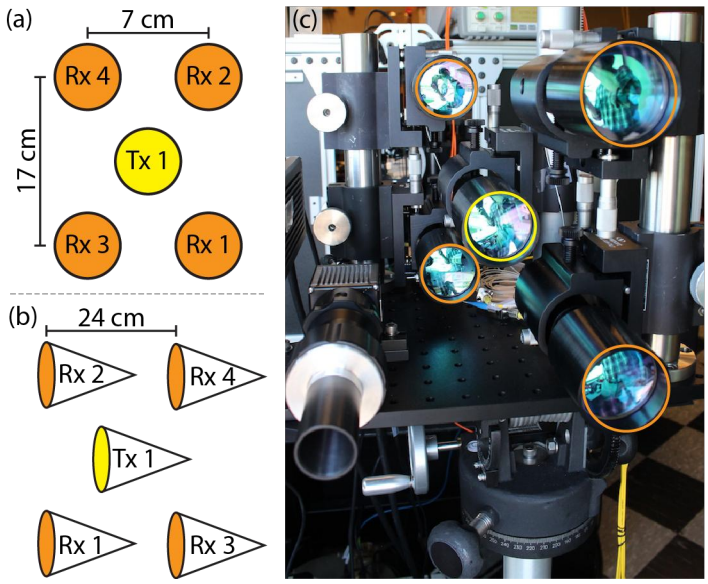

Figure 3: Transmit and receive aperture orientation for bidirectional link as viewed (a) head on, and (b) from the side. (c) Photo of optical module.

The experimental setup in Figure 2 enabled measurements of a CW signal in a double-pass link using the Tx Laser. After propagation through free-space, the received signals were measured by all four receive chains. For these measurements, the digital oscilloscope sample rate was set to 100 MSamples/s to enable capturing of 2.5 seconds of data per acquisition, which was sufficient to capture many uncorrelated states of the atmosphere. Coherent combining was then implemented in offline DSP, as described in Section 3.2.

Figure 3 shows the orientation of the transmit and receive apertures used for the double-pass link, which are all identical 40-mm apertures. The four receive apertures were set up in a grid surrounding the transmit aperture (Figure 3a). Figure 3c shows that Rx 1 and Rx 2 were set up 24 cm in front of Rx 3 and Rx 4. This separation is arbitrary and was done intentionally to emphasize that multi-aperture digital coherent combining does not necessitate precise relative alignment of the receive apertures since relative delays between the received signals can be removed in DSP after down-conversion to the IF via simple correlation. Figure 3c shows a photo of the assembled optical module. The four receive apertures did not include any high-order adaptive optics (AO) or tip and tilt correction. Losses due to the lack of high-order AO were considered to be negligible due to the small size of the apertures used. Any penalties from the lack of tip and tilt correction manifested as fading at the coherent receivers.

3.2 Digital Signal Processing

In the notation of Section 2, the experimental arrangement consisted of a baseband waveform $x(t) = 1$ (i.e., no data modulation), $K = 4$ receiver chains, and a sampling rate of $1/T_s = 100$ MSamples/s.

The primary DSP objective was to implement a maximal ratio combining algorithm. To demonstrate the combining performance, additional signal processing steps were required to appropriately estimate the time-varying SNR of the individual received signals and the composite signal.

Both the coherent combining and the SNR estimation algorithms were applied to non-overlapping signal blocks of N_c samples. Increasing N_c reduces the variance of the estimators, but it also increases the estimator bias considerably when the block duration $N_c T_s$ is comparable to the coherence time of the atmospheric channel. The coherence time was estimated in DSP to be on the order of 5-10 ms. A suitable variance-bias tradeoff was reached by setting $N_c = 10^4$ samples (which gave $N_c T_s = 0.1$ ms).

The maximal ratio combining algorithm was the following (see Ref. 10 for the derivation and justification). A block $B_0 = \{n_0, \ldots, n_0 + N_c - 1\}$ of N_c samples of each of the K received signals can be written as a "data matrix" Y:

$$Y = [\mathbf{y}[n_0], \ldots, \mathbf{y}[n_0 + N_c - 1]] \in \mathbb{C}^{K \times N_c} \tag{10}$$

The weight vector $\mathbf{w}$ is taken to be the complex conjugate of the principal eigenvector of the matrix YY^H, where $(\cdot)^H$ denotes conjugate transpose; the principal eigenvector is the one corresponding to the eigenvalue of largest magnitude. The corresponding composite signal block is then

$$z[n] = \mathbf{w}^T \mathbf{y}[n], \quad n \in B_0. \tag{11}$$

Like the maximal ratio combining algorithm, the SNR estimation was performed in blocks to take advantage of the relative constancy of the atmosphere over a block of size N_c. Consider the signal model for $y_k[n]$ in (1) and the block B_0. First, the intermediate frequency ω and phase noise $\phi[n]$ over the block are estimated to form an estimate $\hat{c}[n]$ of $c[n]$, the signal at the intermediate frequency. Frequency and phase correction is applied by forming

$$\tilde{y}_k[n] = \overline{\hat{c}[n]} \cdot y_k[n], \quad n \in B_0. \tag{12}$$

The sample mean $\widehat{h}_k$ and sample variances $\widehat{\sigma^2_{k,\text{real}}}$ and $\widehat{\sigma^2_{k,\text{imag}}}$ of the block $\{\tilde{y}[n]\}_{n \in B_0}$ are then taken as point estimates of $\{h_k[n]\}_{n \in B_0}$ and the noise variances in each dimension, respectively. Finally, the point estimate of the SNR $\{\rho_k[n]\}_{n \in B_0}$ of the block is defined as

$$\widehat{\rho_k} = \frac{|\widehat{h}_k|^2}{\widehat{\sigma^2_{k,\text{real}}} + \widehat{\sigma^2_{k,\text{imag}}}}. \tag{13}$$

The estimator of the SNR of the composite signal follows identical steps.

4. EXPERIMENTAL RESULTS

This section presents the digital signal processing results of the atmospheric link experiment. Figure 4a shows a 100-ms snapshot of the 2.5-s time-series of the SNR of the four received signals and the composite signal after maximal ratio combining. Table 1 lists the estimated average SNR of the four received signals, the composite signal, and the sum of the constituent SNRs. The averages are formed by taking the time-average of the estimated SNRs. The maximal ratio combining performed well, as evidenced by the small 0.2-dB gap between the average SNR of the composite signal and sum of the constituent average SNRs. The variability in average SNR among the receivers (most apparent between Rx 2 and Rx 4) is most likely due to pointing errors and differences in path losses. Nonetheless, near-lossless combining of the received signals was achieved.

Figure 4b shows the empirical cumulative distribution function (CDF) of the SNR time-series of the individual and composite signals after normalizing by their respective average SNRs. This CDF is the fraction of time that the SNR faded to a given fraction of the average SNR. For example, it can be seen in Figure 4b that for the individual received signals, fades of 20 dB occurred about 1% to 5% of the time, depending on the choice of receiver.* On the other hand, for the composite signal, fades of 20 dB from the mean did not occur during the 2.5-s acquisition. In general, the gap between the individual CDFs and the composite CDF demonstrates that the experimental arrangement achieved a level of spatial diversity. Although we do not discuss it here, spatial diversity has a positive impact on communication system performance; in particular, the benefits of spatial diversity can be evaluated in terms of decreased outage probability or increased fading channel capacity.[11]

*We note that these fade distributions can vary substantially depending on the time of day, temperature, and local wind speed. On the day of the acquisition, a nearby weather station reported 55°F, 6 mph wind, and sunny.

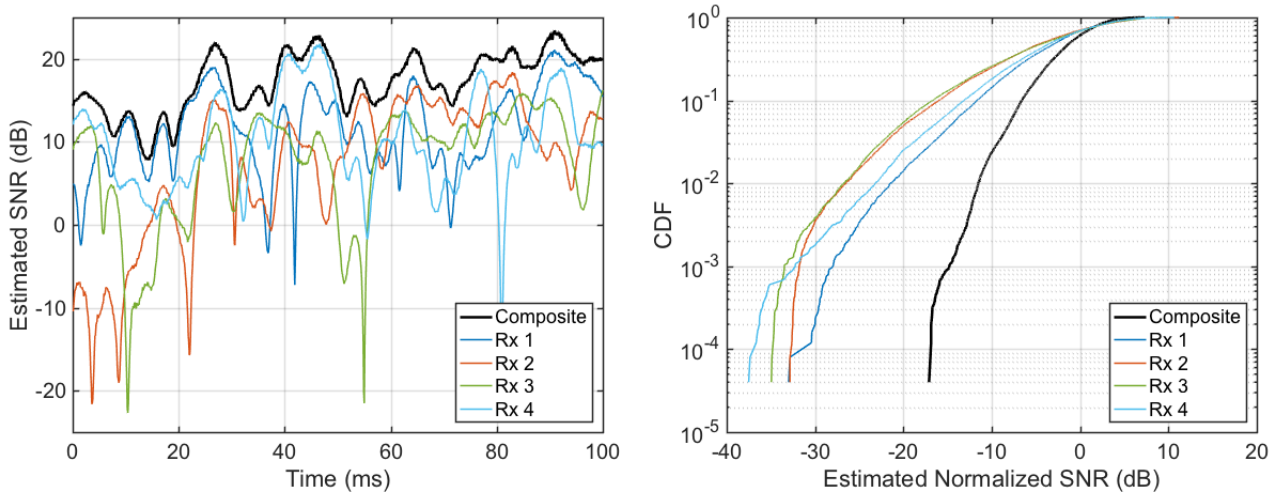

Figure 4: (a) Time-series of SNR as estimated in DSP using a 0.1-ms block-averaging time. A 100-ms snapshot of the full 2.5-s acquisition is shown. (b) Cumulative distribution function of normalized SNR.

Table 1: Estimated average SNR of various signals.

Signal	Estimated Average SNR (dB)
Rx 1	11.7
Rx 2	9.9
Rx 3	12.0
Rx 4	14.5
Composite signal	18.1
Sum of constituent SNRs	18.3

5. CONCLUSION

In summary, this paper presented a system architecture model for analyzing SIMO communication through a fading channel for optical communication. Within that framework the procedure for coherently combining multiple signals after down-conversion and digitization into a composite signal was described. Furthermore, it was shown that maximal ratio combining, a technique that maximizes the SNR of a composite signal, can be implemented given knowledge of the fading process. An experimental demonstration showed that multi-aperture coherent combining could be implemented with negligible losses over a 3.2-km atmospheric link. Additionally, the experimental results provided evidence of the positive impact of spatial diversity on system performance. In the future, a more detailed analysis of the impact of spatial diversity will be considered. Finally, the results of this paper provide evidence for the practicality of using digital coherent aperture combining to increase the capability of optical ground stations for high-rate or deep-space optical communication in the presence of atmospheric fading.

REFERENCES

[1] M. Gregory, D. Troendle, G. Muehlnikel, F. Heine, R. Meyer, M. Lutzer, and R. Czichy, "Three years coherent space to ground links: performance results and outlook for the optical ground station equipped with adaptive optics," *Proc. SPIE* **8610**, p. 861004, 2013.

[2] D. M. Boroson, B. S. Robinson, D. V. Murphy, D. A. Burianek, F. Khatri, J. M. Kovalik, Z. Sodnik, and D. M. Cornwell, "Overview and results of the Lunar Laser Communication Demonstration," *Proc. SPIE* **8971**, p. 89710S, 2014.

[3] H. Takenaka, Y. Koyama, M. Akioka, D. Kolev, N. Iwakiri, H. Kunimori, A. Carrasco-Casado, Y. Munemasa, E. Okamoto, and M. Toyoshima, "In-orbit verification of small optical transponder (SOTA): evaluation of satellite-to-ground laser communication links," *Proc. SPIE* **9739**, p. 973903, 2016.

[4] H. P. Stahl, "Survey of cost models for space telescopes," *Optical Engineering* **49**(5), p. 053005, 2010.

[5] D. J. Geisler, T. M. Yarnall, M. L. Stevens, C. M. Schieler, B. S. Robinson, and S. A. Hamilton, "Multi-aperture digital coherent combining for free-space optical communication receivers," *Optics Express* **24**(12), pp. 12661–12671, 2016.

[6] T. Williams, R. J. Murphy, F. Walther, A. Volpicelli, B. Wilcox, and D. Crucioli, "A free-space optical terminal for fading channels," *Proc. SPIE* **7464**, 2009.

[7] L. C. Andrews, R. L. Phillips, C. Y. Hopen, and M. A. Al-Habash, "Theory of optical scintillation," *J. Opt. Soc. Am. A* **16**(6), pp. 1417–1429, 1999.

[8] D. H. Rogstad, A. Mileant, and T. T. Pham, *Antenna arraying techniques in the deep space network*, John Wiley & Sons, 2005.

[9] D. G. Brennan, "Linear diversity combining techniques," *Proceedings of the IRE* **47**(6), pp. 1075–1102, 1959.

[10] K.-M. Cheung, "Eigen theory for optimal signal combining: a unified approach," *The Telecommunications and Data Acquisition Progress Report 42-126, April–June 1996*, Jet Propulsion Laboratory, Pasadena, California, 1996.

[11] E. Biglieri, J. Proakis, and S. Shamai, "Fading channels: information-theoretic and communications aspects," *IEEE Transactions on Information Theory* **44**(6), pp. 2619–2692, 1998.